

DOI: 10.17725/rensit.2020.12.361

Effect of masses of active layers of C₆₀-4-methylphenylhydrazone N-isoamylisatin fullerene heterostructures on their rectifying characteristics

Alim S.-A. Mazinov, Andrey S. Tyutyunik, Vladimir S. Gurchenko, Veronika Yu. Ilina
V.I. Vernadsky Crimean Federal University, <https://cfuv.ru/>
295007 Simferopol, Russian Federation

E-mail: mazinovas@cfuv.ru, real-warez@mail.ru, gurchenko_v@mail.ru, nika.ilyina@mail.ru

Received June 21, 2020; peer reviewed June 29, 2020; accepted July 06, 2020

Abstract: An organocarbon heterostructure consisting of thin films of fullerene and 4-methylphenylhydrazone N-isoamylisatin was obtained from a solution by irrigation. The procedure for obtaining the samples, the microscopy, and synthesis of the initial powder material have been described. The results of an alternate X-ray phase analysis of the substances used has been presented. The analysis of changes in the electrical and optical characteristics of the active layers, depending on the mass of the solid phase has been carried out. The relationship between a sequential increase in film thickness and an increase in the absorption coefficient of infrared electromagnetic radiation has been revealed. Having determined the optimal thicknesses of the active layers of the heterostructure, based on fullerene C₆₀ and 4-methylphenylhydrazone N-isoamylisatin, we achieved an increase in photoconductivity by two orders of magnitude. The obtained light current – voltage characteristics of such thin-film structures are rectilinear in nature with a direct load of up to 10 V.

Keywords: thin-film structures, fullerene, isatin, photoelectric effect, x-ray phase analysis, current-voltage characteristics

PACS 61.48.+c, 61.66.Hq, 73.61.-r

Acknowledgements: The reported study was funded by RFBR, project number 19-32-90038. The authors are grateful to the company “MCT-nano” for providing the source material C₆₀.

For citation: Alim S.-A. Mazinov, Andrey S. Tyutyunik, Vladimir S. Gurchenko, Veronika Yu. Ilina. Effect of masses of active layers of C₆₀-4-methylphenylhydrazone N-isoamylisatin fullerene heterostructures on their rectifying characteristics. *RENSIT*, 2020, 12(3)361-368. DOI: 10.17725/rensit.2020.12.361.

CONTENTS

1. INTRODUCTION (361)
 2. SYNTHESIS OF ACTIVE LAYERS AND X-RAY PHASE ANALYSIS (362)
 3. PRECIPITATION AND MICROSCOPY OF THIN FILMS (363)
 4. MID-WAVE IR ABSORPTION SPECTRA (364)
 5. CURRENT-VOLTAGE CHARACTERISTICS OF THIN FILMS (365)
 6. CONCLUSION (366)
- REFERENCES (367)

1. INTRODUCTION

The global trend in the development of the field of optoelectronic molecular compounds has led to an expansion of the functional characteristics of new photovoltaic materials. Since one of the most important factors determining the low conversion efficiency of thin-film-based solar cells is low absorption, many modern studies are aimed at identifying various ways to improve this parameter [1]. One of these areas is the construction of

devices with the use of organic materials. Organic electronics is gaining popularity due to the low cost of manufacture, the reduction in the weight of materials [2] and the feasibility of producing devices with a larger surface area using flexible substrates [3]. Recent developments in the field of photovoltaics have made it possible to obtain organic solar cells with an efficiency of $> 11\%$ [4,5]. Solar energy is not the only area of application of organic materials. Organic field effect transistors (OFET) over the past 5 years have been widely used due to the control of the initial chemical composition of the substance [6,7]. In particular, OFETs using carbon materials (fullerenes) as a basis are effectively used due to the high electron mobility ($11 \text{ cm}^2 \text{ V}^{-1}\text{s}^{-1}$) [8]. The use of fullerene as a transport layer for electrons improves the electrical characteristics of organic light emitting diodes (OLEDs) [9].

Over the past decades, isatin derivatives have established themselves as affordable photochromic materials [10,11] with the ability to reradiate the ultraviolet spectrum in the visible range [12]. The ease of the molecular composition rearrangement of isatins enables one to control the change in their physical properties. The use of isatin derivatives in photovoltaics made it possible to obtain an efficiency coefficient of more than 9% [13]. In turn, fullerene appears as a relatively strong electron acceptor with n-type conductivity

[14]. The use of various modifications of hydrazone and isatin derivatives as an effective donor made it possible to improve the characteristics of photoconverting elements with a bulk heterojunction.

On the basis of the foregoing, the purpose of this paper was defined as follows: to study the effect of an electromagnetic wave of the optical range on the rectifying properties of organo-carbon heterostructures when changing the thickness of active layers, as well as to determine the optimal mass of the substance needed to obtain the maximum increase in direct currents of the structures under study.

2. SYNTHESIS OF ACTIVE LAYERS AND X-RAY PHASE ANALYSIS

The synthesis of the organic precursor was carried out with the technique similar to the one presented by Cigan [15]. The starting N-isoamylisatin weighing 2.03 g (0.01 mmol) was dissolved in methanol, the volume of which was 50 ml, in the process of stirring and heating. Next, 4-methylphenylhydrazine weighing 1.35 g (0.011 mmol) was added to the solution. The mixture was boiled for 1-2 hours until a precipitate formed, the mixture being constantly stirred. The end products were isolated by filtration and purified by recrystallization from ethanol. As a result of the synthesis, 2.4 g of the end product were obtained with the yield of 73%. The purity and structure of the compounds were confirmed by ^1H NMR spectroscopy and

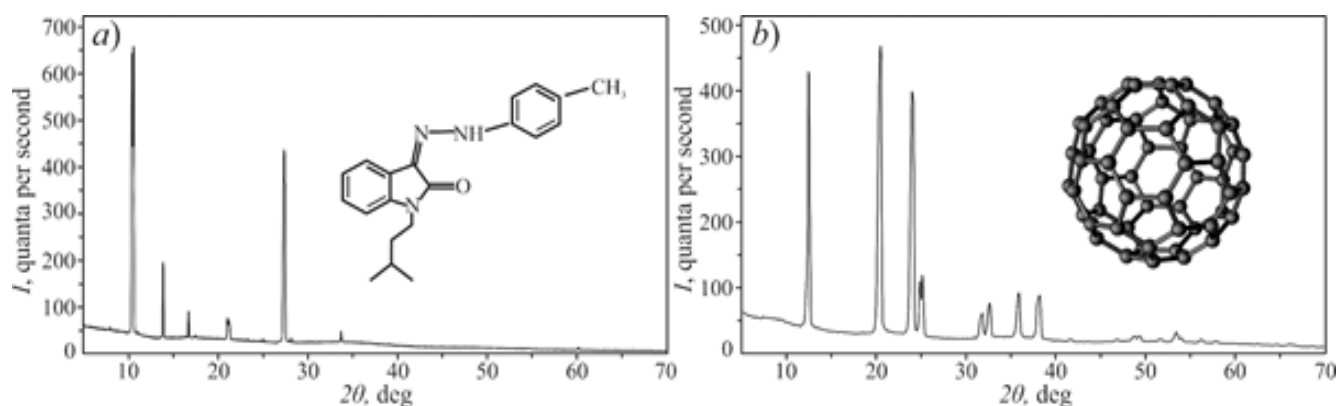


Fig. 1. X-ray diffraction patterns of organic isatin (a) and fullerene (b) in the solid phase.

elemental analysis. The source/initial fullerene C₆₀ was provided by ‘MST nano’ company, with 99.5% purity.

The determination of the phase purity of the initial organic and carbon materials in the solid phase was carried out using the method of X-ray phase analysis. The diffraction patterns were recorded on a DRON-3 general-purpose diffractometer (Bragg-Brentano focusing scheme using a graphite monochromator) in the angular region 2θ from 5° to 70°, using an X-ray tube with a copper anode λ (Kα) = 0.154184 nm. The detector rotation speed was - 0.5°/min, with a constant time equal to - 1·10³ pulses per second. The primary and secondary bundles were limited by slits: horizontal — 0.25 mm, vertical — 6 mm, and Soller slits — 0.5 mm. The rotation speed of the sample is 120 revolutions per minute (the axis is in the survey plane).

According to the results of X-ray phase analysis, 4-methylphenylhydrazone N-isoamylisatin in the solid phase showed that this organic material has tetragonal syngony with the sides: a = 19.27 Å; b = 19.27 Å; c = 14.14 Å; and it belongs to space group I -4 2 m with angles α = 90°; β = 90°; γ = 90°. Observations of Fullerene C₆₀ in the solid phase confirmed its molecular composition. The carbon material has a cubic syngony with the sides: a = 14.17 Å; b = 14.17 Å; c = 14.17 Å and the spatial group Fm 3 is aligned at angles: α = 90°; β = 90°; γ = 90°.

3. PRECIPITATION AND MICROSCOPY OF THIN FILMS

After confirming the initial composition of the substance by X-ray phase analysis, further studies were carried out directly with carbon and organic thin films. The formation of film structures based on powder fullerene C₆₀ and 4-methylphenylhydrazone N-isoamylisatin was carried out by the method of irrigation from solution [16]. Non-aromatic compounds were used as solvents: dichloromethane for fullerene and chloroform for isatin. The fixed concentration of the starting material solid phase in the solution was 0.5 mg/ml. To assess the uniformity of the films surface and to detect neoplasms, the starting materials in the solution were deposited on dielectric substrates of 18×18 mm. geometric dimensions. The relief of the films was analyzed by transmission and reflected microscopy with the use of LOMO Mii-4M microinterferometer with additional illumination by a semiconductor laser and an extended optical path to a camera with a 1/2FF 10MP matrix (Fig. 2). To determine the optimal mass of the starting materials, five variations of the experimental samples were formed. The gradual increase in the mass of isatin (Fig. 2a-e) and C₆₀ (Fig. 2k-o) from 0.15 to 0.75 mg in increments of 0.15 mg made it possible to dynamically evaluate the change in the geometry of the film and the material distribution on the surface of organic structures.

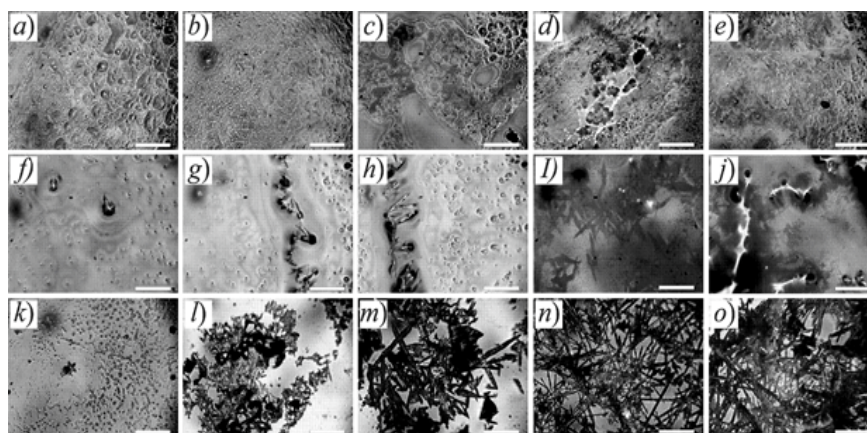


Fig. 2. Microphotographs of isatin films: (a - 0.15 mg; b - 0.3 mg; c - 0.45 mg; d - 0.6 mg; e - 0.75 mg), transition layer (f - 0, 15 mg; g - 0.3 mg; h - 0.45 mg; I - 0.6 mg; j - 0.75 mg) and fullerene films (k - 0.15 mg; l - 0.3 mg; m - 0.45 mg; n - 0.6 mg; o - 0.75 mg). The line length is 50 microns.

As a result, the surface analysis showed that an increase in the mass of the starting material is clearly accompanied by a change in the surface morphology. Isatin films deposited with chloroform (CHCl_3) can be described as relatively uniform. Initially, with a starting material mass of 0.15 mg (Fig. 2 a), the film surface has an island-like (dispersed) appearance with a thickness of 500–600 nm. With an increase in the mass of the substance up to 0.3 mg (Fig. 2b), the formation of bonds between the “islands” is observed. The thickness of such films is 600–700 nm. A further increase in the amount of the starting material leads to a complete (continuous) coating of the entire surface of the substrate (Fig. 2c-e). This fact is accompanied by a significant increase in the thickness of the films: with masses of 0.45, 0.6, and 0.75 mg, the thickness is 2.2–2.3 μm 3–3.1 μm and 3.6–3.7 μm , respectively.

Fullerene films deposited with dichloromethane (CH_2Cl_2) are characterized by relative surface heterogeneity. With a mass of 0.15 mg of the starting material (Fig. 2k), the appearance of individual “point” particles with sizes of 1–3 μm is observed. Moreover, the film thickness is 300–400 nm. A sequential increase in matter to 0.3 and 0.45 mg (Fig. 2l,m) is characterized by an increase in various agglomerations, and the initial formation of “star-shaped” structures with sizes of “rays” reaching 30–40 μm is also traced. The thickness of such films increases to 400–500 and 500–600 nm, respectively. With an increase in mass to 0.6 and 0.75 mg (Fig. 2n,o), complete volumetric overlap of the surface with carbon “star-shaped” structures organized by self-assembly is observed, the sizes of which reach about 40–50 μm . In this case, the thickness increases to 600–700 nm for 0.6 mg and 700–800 nm for 0.75 mg. The fullerene-isatin transition layer has a mixed surface morphology (Fig. 2f-j), where C_{60} molecules are formed into separate cores.

4. MID-WAVE IR ABSORPTION SPECTRA

Given the specifics of the microobjects formation by self-assembly, the next step was to conduct a study using IR spectroscopy. This method was used to determine the possible changes in the molecular composition of the obtained thin films. The interaction of medium-wave IR radiation and carbon and organic material was studied using an Agilent Cary 630 FTIR IR Fourier spectrometer with an attenuated total internal reflection (ATR) attachment in the spatial frequency range of 650–4000 cm^{-1} and a resolution of 4 cm^{-1} . For the convenience of analyzing the interaction of infrared electromagnetic waves and carbon and organic films, the intervals: 650–1250 cm^{-1} , 1250–1850 cm^{-1} and 2650–3250 cm^{-1} were separately set.

When studying the spectral dependences of the mid-wave IR range, it is necessary to note a significant number of absorption peaks in the organic film, which is due to the complexity of the structure of the 4-methylphenylhydrazone molecule of N-isoamylisatin (Fig. 3a). In the region of small wavelengths of 2650–3250 cm^{-1} , peaks were observed associated with vibrations of the C–H and N–H atom groups. Peaks observed due to the presence of C=O and C=N bonds, were detected in the frequency interval 1250–1850 cm^{-1} . Besides, the C=O bond stretching vibrations, in the range of 1630–1740 cm^{-1} , assign the substance to the amide class I. The peak at the wavelength of 1612 cm^{-1} is associated with the N–H bending vibration and the N–C=O stretching vibration, which is characteristic of the amide class II. The main contribution to the absorption of the IR electromagnetic wave, in the region 1364–1610 cm^{-1} , is made by stretching vibrations C=C of benzene rings. The 650–1250 cm^{-1} region was distinguished by the sequence of absorption maxima, which are caused by the action of deformation and stretching vibrations of groups of C–N, C–C, C–H atoms. It is worth

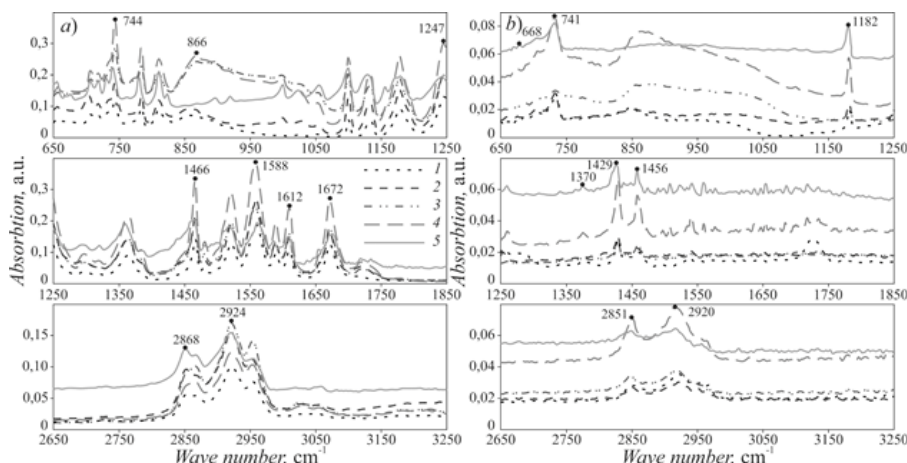


Fig. 3. IR optical absorption spectra of Isatin (a) and Fullerene (b) films, with masses: 1) 0.15 mg; 2) 0.3 mg; 3) 0.45 mg; 4) 0.6 mg; 5) 0.75 mg.

noting the significant contribution of bending vibrations of C–H groups in benzene rings and an alkyl substituent in the frequency range 744–1128 cm⁻¹.

The analysis of carbon films in the IR range, for different masses of the substance, showed the presence of a significantly smaller number of absorption peaks compared to organic films (Fig. 3b). This is due to the more uniform structure of the fullerene molecule. In the frequency range 2650–3250 cm⁻¹, a double peak of low intensity is observed, which is typical of the C_{sp3}-H bond in higher hydrocarbons. Also, this connection is characterized by the presence of an absorption band at the frequency of 1370 cm⁻¹. The peaks, that characterize the obtained carbon films as fullerene, are present at frequencies of 1182 and 1429 cm⁻¹, and the absorption band at the frequency of 1429 cm⁻¹ coalesces with the band from the alkyl group of 1456 cm⁻¹. Feebly marked absorption bands in the regions of 1649–1659 cm⁻¹ are specific to the C=O group vibrations. The presence of methane chlorine derivatives at the wave numbers of 668 cm⁻¹ and 741 cm⁻¹ is due to the use of dichloromethane (CH₂Cl₂) as a solvent for fullerene.

Integrating data on the diversity of the medium-wave IR interaction spectrum, it can be noted that an increase in the mass of functional layers practically does not affect the shape and shift of the absorption peaks. However, an

increase in the intensity of absorption peaks with an increase in the amount of substance is clearly traced, which indicates the formation of a greater number of intermolecular bonds and the formation of a more uniform absorbing layer, which is characteristic of the starting material.

5. CURRENT-VOLTAGE CHARACTERISTICS OF THIN FILMS

To determine the optimal mass of active layers in order to improve their transforming properties, we studied the heterostructure based on C₆₀ fullerene and N-isoamylisatin 4-methylphenylhydrazone. Electrodynamic parameters were investigated using a Keysight B1500A semiconductor analyzer. The measurements were carried out at least 10 times at room temperature, followed by averaging. To evaluate photoactivity, we used a LED matrix with a flux density of about 300 W/m² and an incoming power of 60 mW. Indium tin oxide (ITO), with a specific resistance of 16–18 Ω/sq, and aluminum deposited on a sital, with the resistance of 20 Ω/sq and the thickness of 120 nm, were used as a contact group. The geometric dimensions of the substrates (Al and ITO) were 10×10 mm. The heterostructure (ITO-isatin-C₆₀-Al) was a “sandwich”, with fullerene deposited on aluminum and isatin deposited on indium tin oxide. The study of the charge kinetics of active

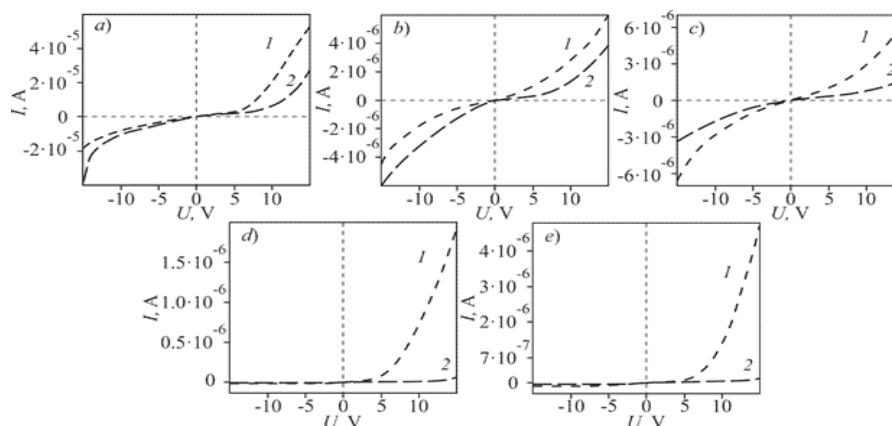


Fig. 4. Light (1) and dark (2) current-voltage characteristics of the ITO-isatin-C60-Al heterostructure, with mass fractions: a - 0.15 mg; b - 0.3 mg; c - 0.45 mg; d - 0.6 mg; e - 0.75 mg.

layers was carried out by measuring the current-voltage characteristics (Fig. 4).

To determine the optimal mass of the starting material, five similar variations of the experimental samples with masses from 0.15 to 0.75 mg were formed. All samples showed photosensitivity. Specifically, for a sample with the mass of 0.15 mg the light current totaled $50.9 \mu\text{A}$ which is 1.87 times as large as the dark one – $27.2 \mu\text{A}$. Doubling of the starting material was accompanied by a slight decrease in photosensitivity up to 1.35 times. A heterostructure with 0.45 mg of the starting material was characterized by the dark current of $18.9 \mu\text{A}$ and the light current of $66.3 \mu\text{A}$, which is an increase in current by 3.5 times. A further increase in the amount of the starting material was accompanied by a significant increase in the kinetics of charge carriers. Thus, for a sample with a mass of 0.6 mg, the current is 91 times greater than the dark CVC, the heterostructure being exposed to irradiation with an electromagnetic wave of the visible range. A 0.75 mg sample showed a 70-fold increase in photocurrent.

The increase in photocurrent with an increase in the bulk density of the active layers can most likely be accounted for by the formation of an extended pseudo-crystalline atomic structure, which provides acceptable conductivity by increasing the mobility of charge carriers directly inside individual

formations - macroparticles. Also, an increase in mass leads to a decrease in the activation energy of the hopping conduction mechanism, thereby increasing the current collection of photoactive charge carriers [17].

6. CONCLUSION

The key result of the study is determination of the substance optimal mass by an experimental way to build a potential barrier on the basis of fullerene and the organic compound 4-methylphenylhydrazone N-isoamylisatin. The microscopic analysis made it possible to demonstrate the phased formation of microstructured objects. The interaction of the IR range electromagnetic radiation and thin-film structures showed that a change in the mass fraction of active layers practically does not affect the shape and shift of the absorption peaks, but leads to an increase in their intensity. This trend can be accounted for by the formation of a uniform absorbing layer and an increasing number of intermolecular bonds. The analysis of heterojunctions photoelectric characteristics, masses of which were 0.6 and 0.75 mg, showed an increase in direct currents by two orders of magnitude, compared with direct currents in samples with masses: 0.15, 0.3 and 0.45 mg. This fact leads us to deduce an inference about the formation of a potential barrier at the isatin – C_{60} interface which is due to the different morphology of basic molecular systems.

REFERENCES

1. Stanculescu A, Breazu C, Socol M, Rasoga O, Preda N, Petre G, Solonaru AM, Grigoras M, Stanculescu F, Socol G, Popescu-Pelin G, Girtan M. Effect of ITO electrode patterning on the properties of organic heterostructures based on non-fullerene acceptor prepared by MAPLE. *Applied Surface Science*, 2020, 145351, doi: 10.1016/j.apsusc.2020.145351.
2. Huttner A, Breuer T, Witte G. Controlling Interface Morphology and Layer Crystallinity in Organic Heterostructures: Microscopic View on C₆₀ Island Formation on Pentacene Buffer Layers. *ACS Appl. Mater. Interfaces*, 2019, 11:35177–35184, doi: 10.1021/acsami.9b09369.
3. Mizukami M, Cho S-I, Watanabe K, Abiko M, Suzuri Y, Tokito S, Kido J. Flexible Organic Light-Emitting Diode Display Driven by Inkjet-Printed High-Mobility Organic Thin-Film Transistors. *IEEE Electron Device Lett*, 2018, 39:39-42.
4. Zhang Y-X, Fang J, Li W, Shen Y, Chen J-D, Li Y, Gu H, Pelivani S, Zhang M, Li Y, Tang J-X. Synergetic Transparent Electrode Architecture for Efficient Nonfullerene Flexible Organic Solar Cells with >12% Efficiency. *ACS Nano*, 2019, 13:4686-4694, doi: 10.1021/acsnano.9b00970.
5. Xie S, Wang J, Wang R, Zhang D, Zhou H, Zhang Y, Zhou D. Effects of processing additives in non-fullerene organic bulk heterojunction solar cells with efficiency >11%. *Chinese Chemical Letters*, 2019, 30(1):217-221, doi:10.1016/j.ccl.2018.04.001.
6. Li H, Shi W, Song J, Jang H-J, Dailey J, Yu J, Katz HE. Chemical and Biomolecule Sensing with Organic Field-Effect Transistors. *Chemical Reviews*, 2019, 119(1):3-35, doi: 10.1021/acs.chemrev.8b00016.
7. Kerfoot J, Korolkov VV, Svatek SA, Alkhamisi M, Taniguchi T, Watanabe K, Parkinson PW, Beton PH. Two-Dimensional Diffusion of Excitons in a Perylene Diimide Monolayer Quenched by a Fullerene Heterojunction. *The Journal of Physical Chemistry C*, 2019, 123(19):12249-12254, doi: 10.1021/acs.jpcc.9b01413.
8. Novikov AV, Leshanskaya LI, Dremova NN, Parfenov A, Troshin P. Environment-friendly aqueous processing of [60]fullerene semiconducting films for truly green organic electronics. *Journal of Materials Chemistry C*, 2020, 8:495-499, doi: 10.1039/c9tc05007h.
9. Han S, Huang C, Lu Z-H. Color tunable metal-cavity organic light-emitting diodes with fullerene layer. *Journal of Applied Physics*, 2005, 97(9):093102, doi: 10.1063/1.1887830.
10. Zheng J, Huang F, Lia Y, Xua T, Xua H, Jia J, Ye Q, Gao J. The aggregation-induced emission enhancement properties of BF₂ complex isatin-phenylhydrazone: Synthesis and fluorescence characteristics. *Dyes Pigments*, 2015, 113:502-509, doi: 10.1016/j.dyepig.2014.09.025.
11. Zheng J, Li Y, Cui Y, Jia J, Ye Q, Han L, Gao J. Isatin-phenylhydrazone dyes and boron complexes with large Stokes shifts: synthesis and solid-state fluorescence characteristics. *Tetrahedron*, 2015, 71:3802-3809.
12. Gusev AN, Shul'gun VF, Topilova ZM, Meshkov SB. Synthesis, structure, and photoluminescence of 5phenyl2pyridyl5,6dihydro[1,2,4]triazolo[1,5c]quinazolines. *Russian Chemical Bulletin, International Edition*, 2012, 61(1):95-98, doi: 10.1007/s11172-012-0014-9.
13. Chocho CL, Spanos M, Katsouras A, Tatsi E, Drakopoulou S, Gregoriou VG, Avgeropoulos A. *Progr. Polym. Sci*, 2019, 91:51-79.
14. Zimirov VM, Zaharova IB. *St. Petersburg Polytechnical State University Journal. Physics and Mathematics*, 2012, 2(146):18-21 (in Russ.).
15. Cigan M, Jakusova K, Gaplovsky M, Filo J, Donovalova J, Gaplovsky A. *Photochemical & Photobiological Sciences*, 2015, 14(11):2064-2073.
16. Starostenko VV, Mazinov AS, Tyutyunik AS, Fitaev ISH, Gurchenko VS. *St. Petersburg*

Polytechnical State University Journal. Physics and Mathematics, 2020, 1(13):106-117.

17. Nikitenko VR, Tyutyunev AP. *Semiconductor Physics and Technology*, 2007, 41(9):1118-1125 (in Russ.).